Science Advances
AAAS

advances.sciencemag.org/cgi/content/full/5/3/eaav8423/DC1

Supplementary Materials for

pH-dependent gating mechanism of the *Helicobacter pylori* urea channel revealed by cryo-EM

Yanxiang Cui, Kang Zhou, David Strugatsky, Yi Wen, George Sachs, Z. Hong Zhou*, Keith Munson

*Corresponding author. Email: hong.zhou@ucla.edu

Published 20 March 2019, *Sci. Adv.* **5**, eaav8423 (2019)
DOI: 10.1126/sciadv.aav8423

The PDF file includes:

Other Supplementary Material for this manuscript includes the following:

(available at advances.sciencemag.org/cgi/content/full/5/3/eaav8423/DC1)

Movie S4 (.mov format). Atomic model and density fit views of 6his*Hp*UreI in open conformation.
Movie S5 (.mov format). 6his*Hp*UreI closed and open conformations morph.

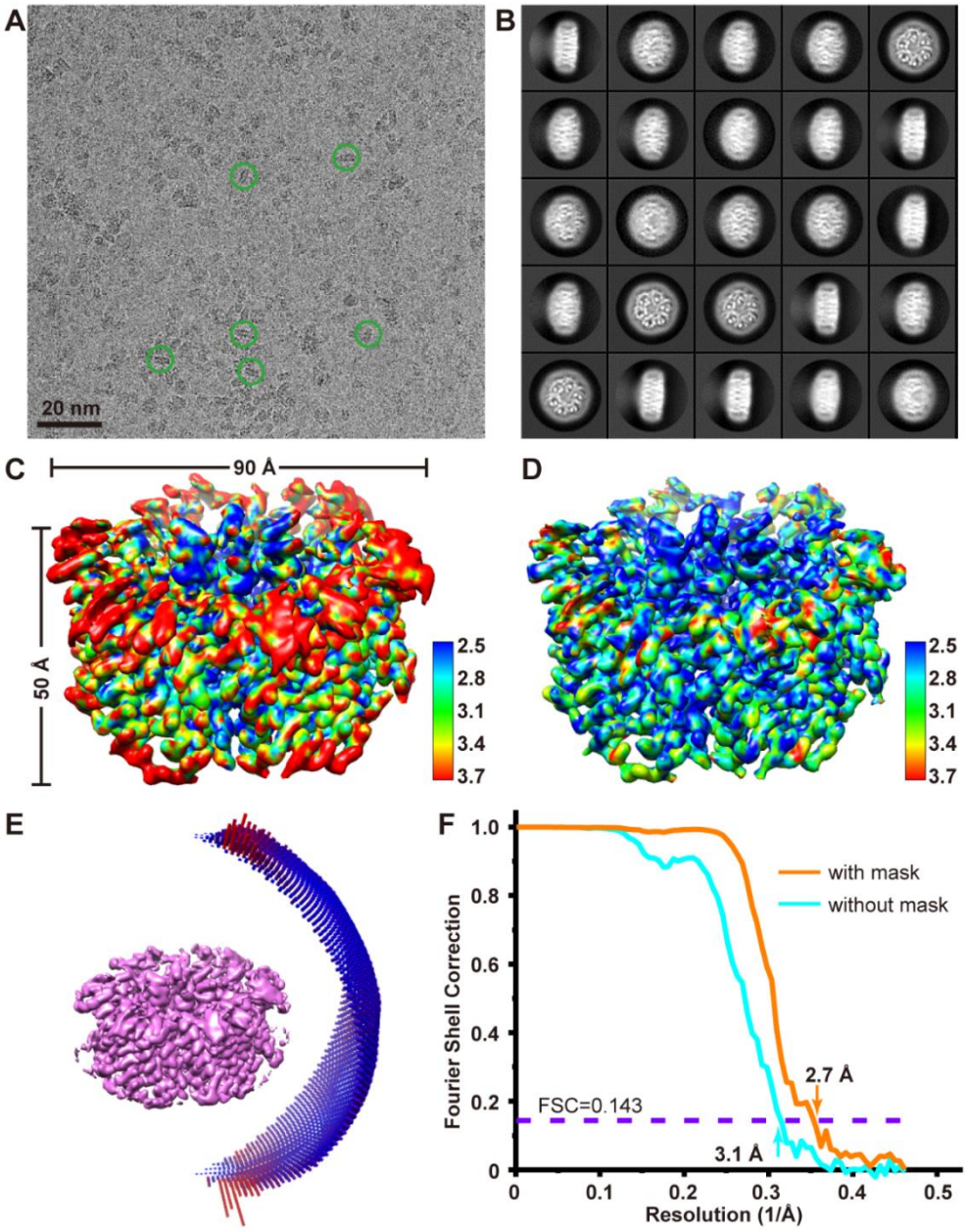

Fig. S1. Cryo-EM analysis of 6his*Hp*UreI in closed conformation. (**A**) A representative cryoEM micrograph of 6his*Hp*Urel in the closed conformation with representative particles circled. (**B**) Representative 2D class averages. (**C** and **D**) The local resolution evaluation of the reconstructed maps without (C) or with (D) a mask. (**E**) Angular distribution. (**F**) Global resolution evaluation based on "gold-standard" Fourier shell correction (FSC) generated by RELION.

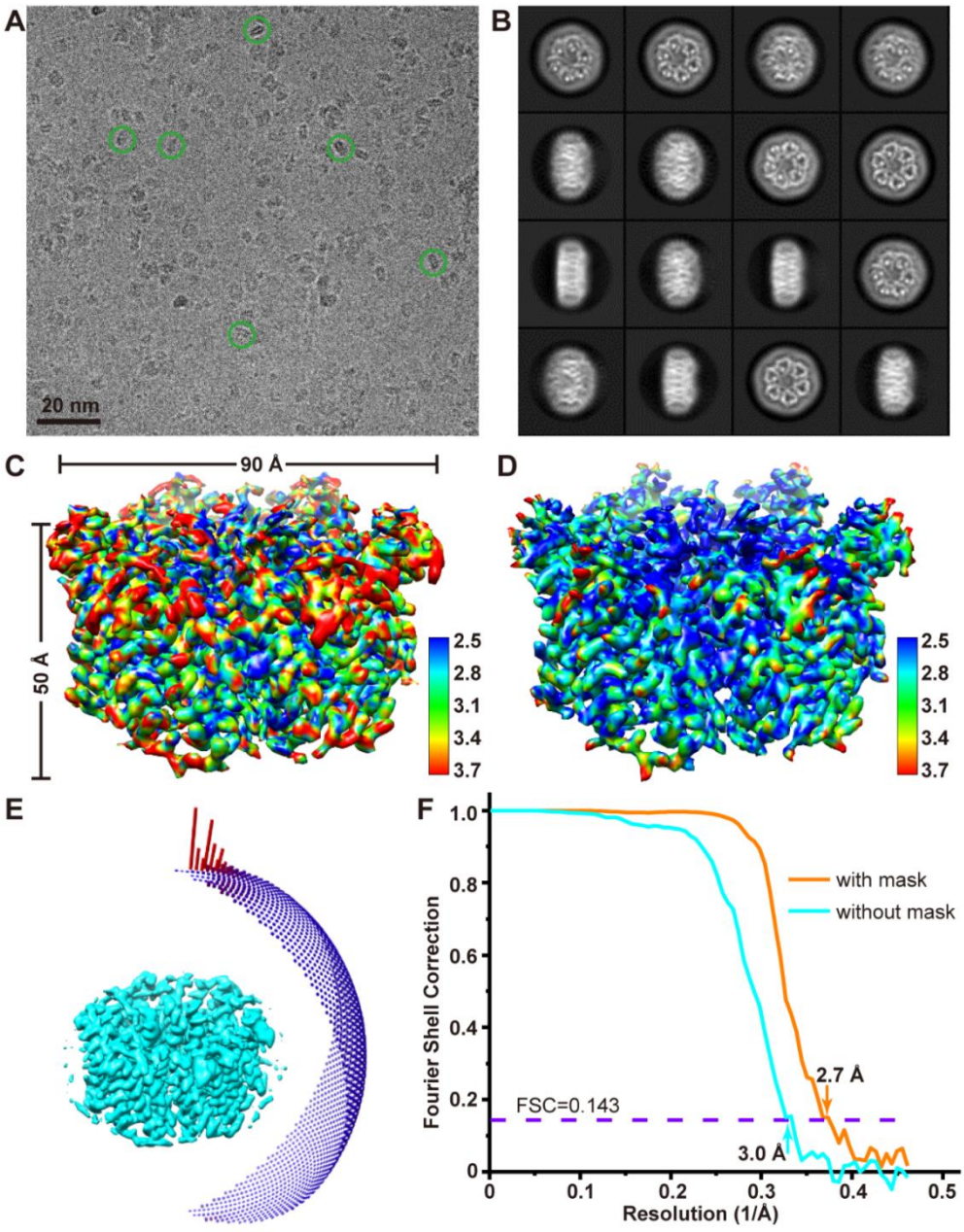

Fig. S2. Cryo-EM analysis of 6his*Hp*UreI in open conformation. (**A**) A representative cryoEM micrograph of 6his*Hp*Urel in the open conformation with representative particles circled. (**B**) Representative 2D class averages. (**C** and **D**) The local resolution evaluation of the reconstructed maps without (C) or with (D) a mask. (**E**) Angular distribution. (**F**) Global resolution evaluation based on "gold-standard" Fourier shell correction (FSC) generated by RELION.

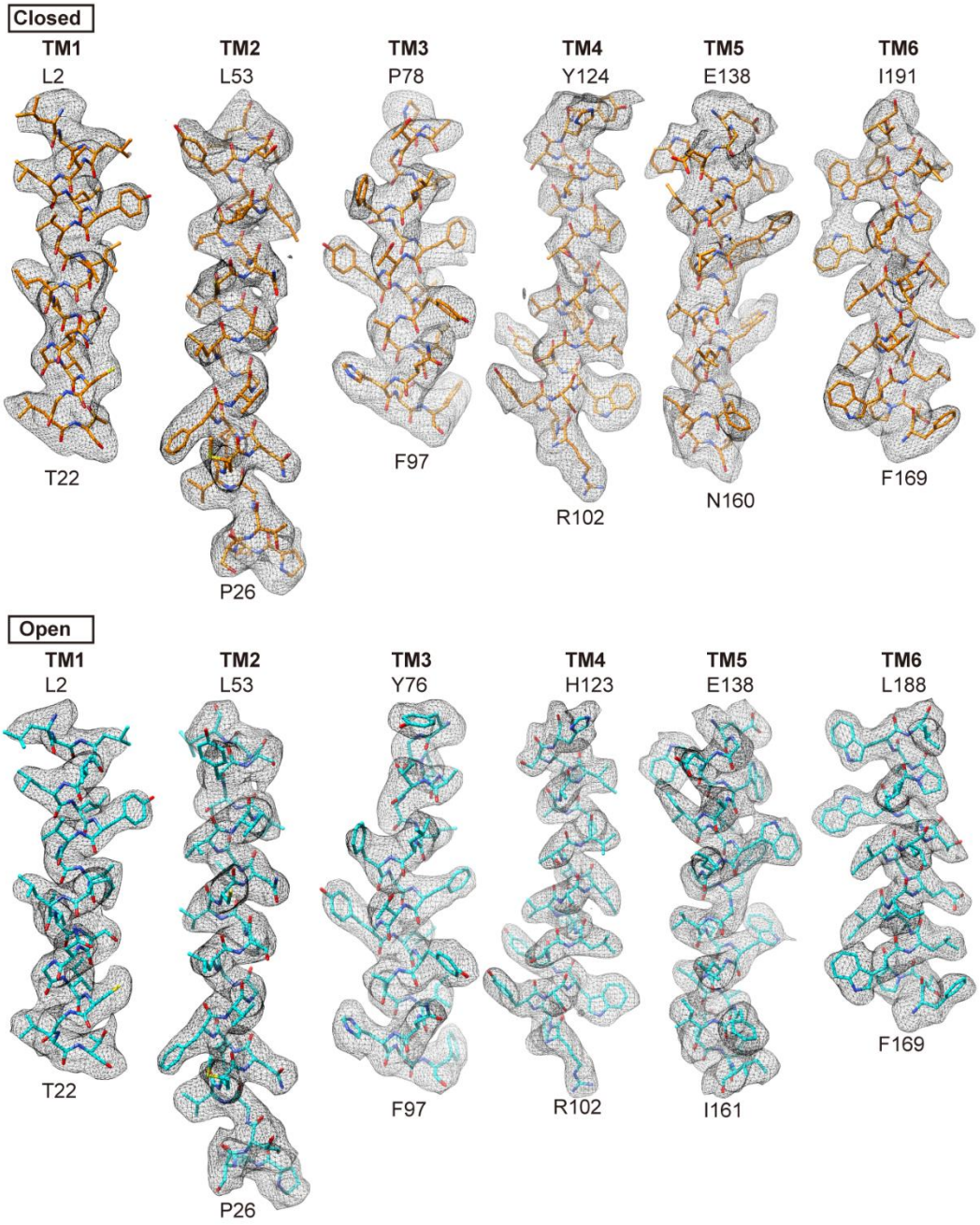

Fig. S3. Cryo-EM densities (mesh) of the six TM helices in 6his*Hp*UreI in the closed and open conformations superposed with their atomic models. The models are shown as sticks colored according to atom type: C, orange (closed) or cyan (open); N, blue; O, red; and S, yellow.

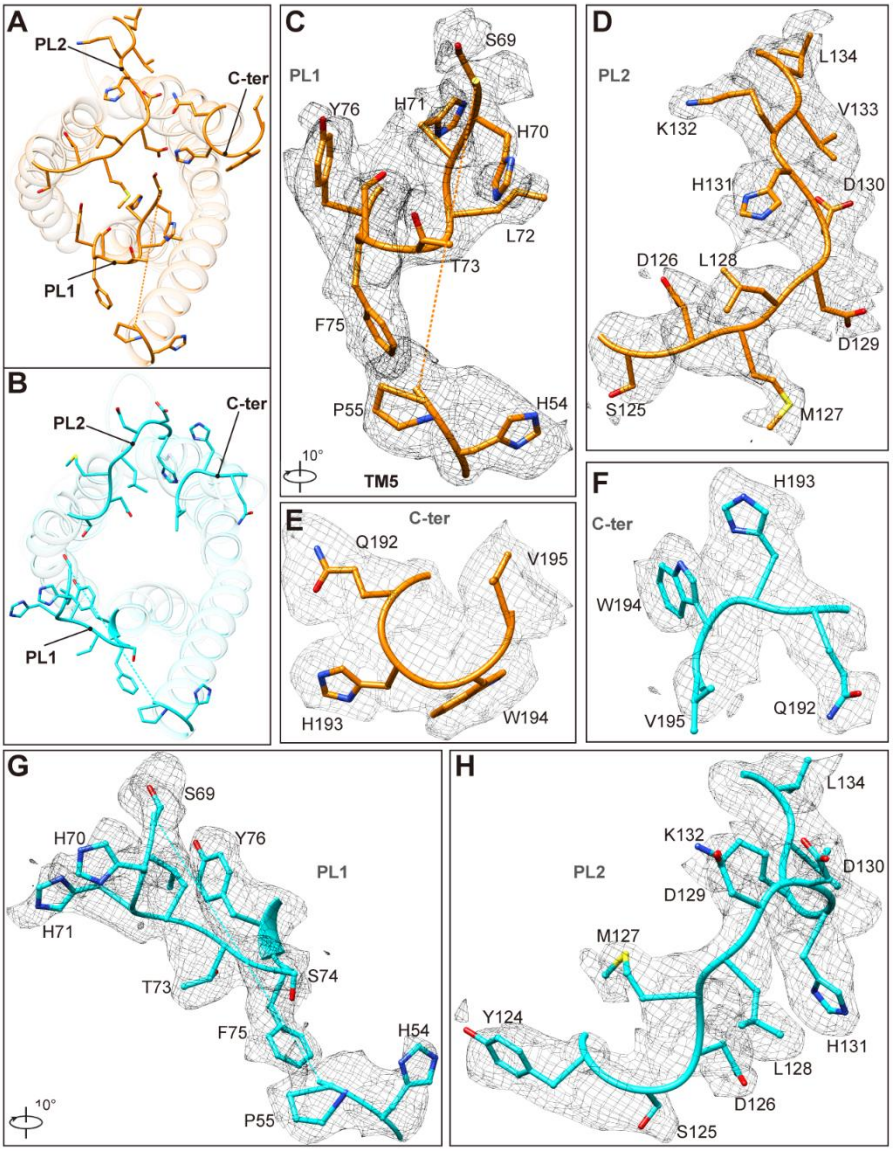

Fig. S4. Details of the cryo-EM densities overlaid with their atomic models (sticks) of the PLs and C terminus in the closed (orange) and open (cyan) conformations. (**A** and **B**) Periplasmic view of one protomer in the closed (A) and open (B) conformations. (**C-E**) PL1, PL2 and C-terminus in the closed conformation. (**F-H**) C-terminus, PL1 and PL2 in the open conformation.

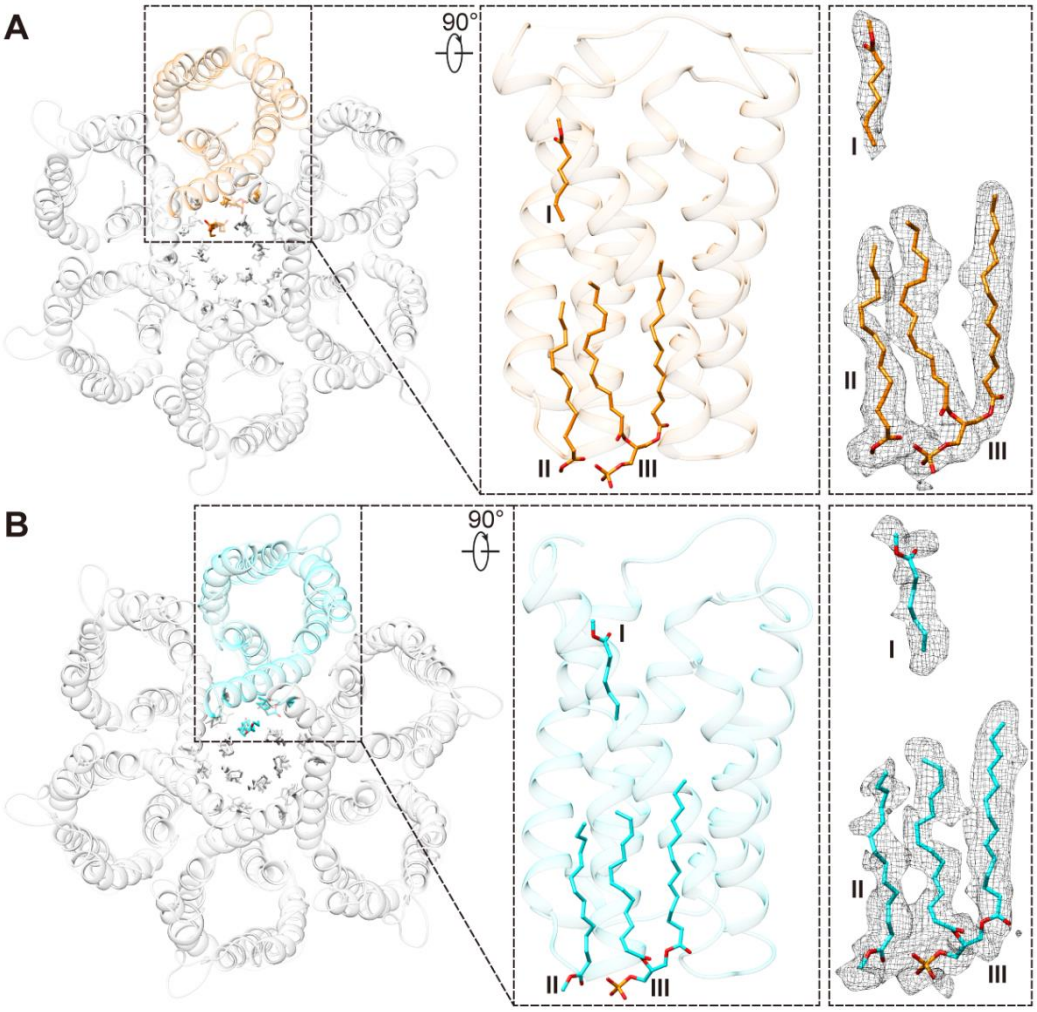

Fig. S5. Ordered lipids resolved in the cryoEM density maps. Ordered lipids resolved in the cryoEM density maps in the closed (**A**) and open (**B**) conformations. The density is shown as grey mesh and the atomic model of the lipids as colored sticks.

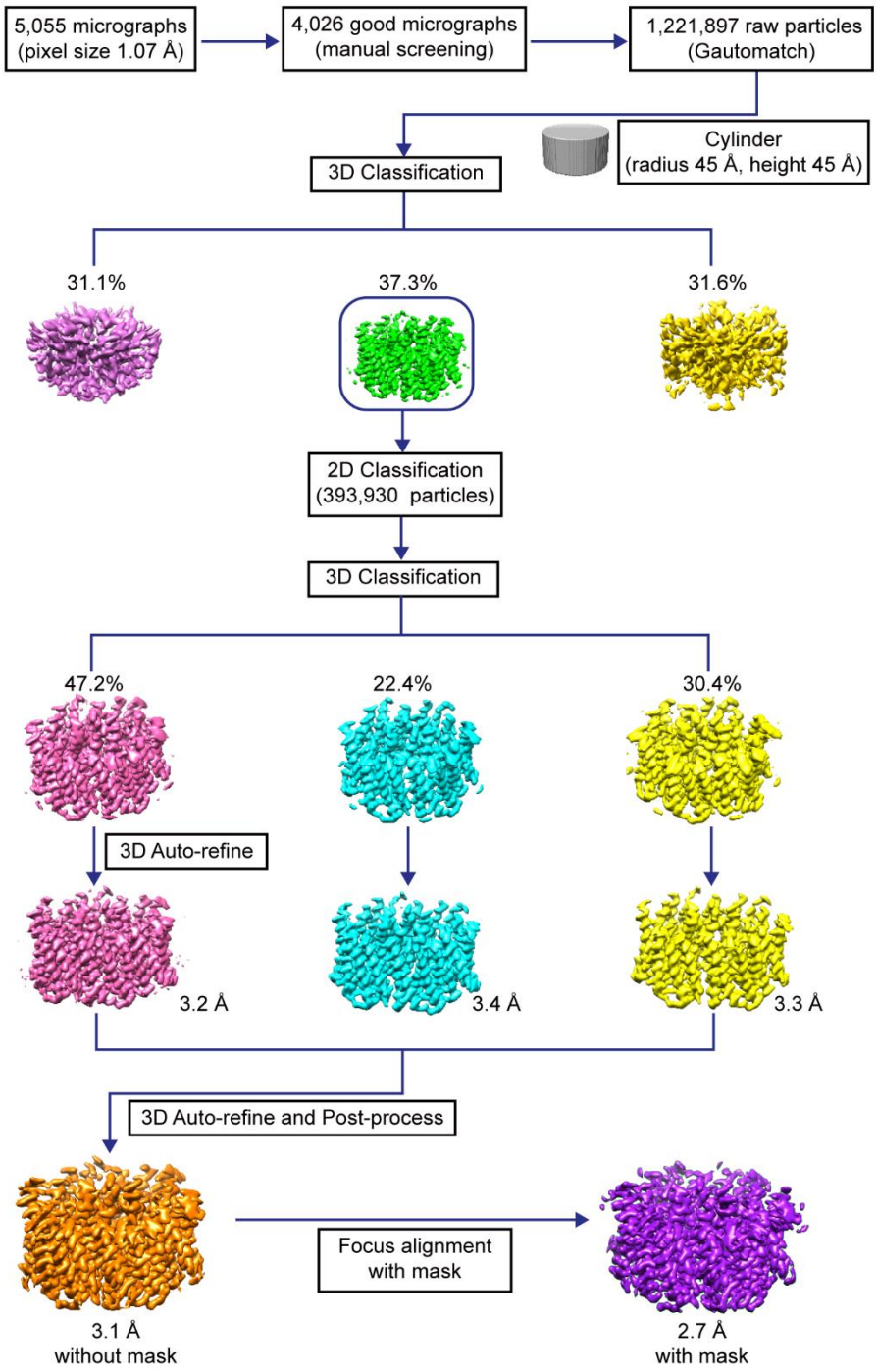

Fig. S6. Data processing workflow used for the dataset recorded for the sample in the closed conformation.

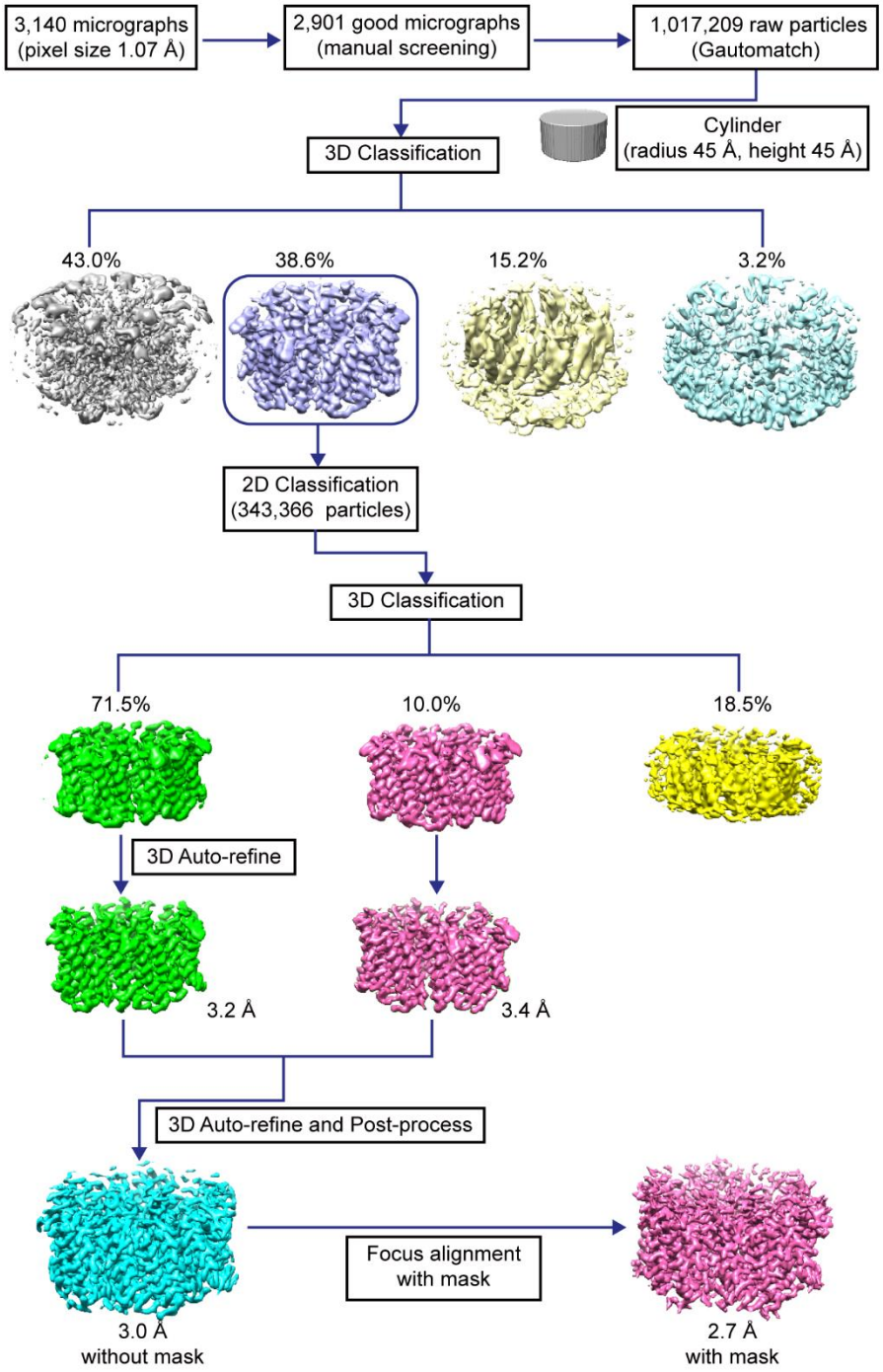

Fig. S7. Data processing workflow used for the dataset recorded for the sample in the open conformation.

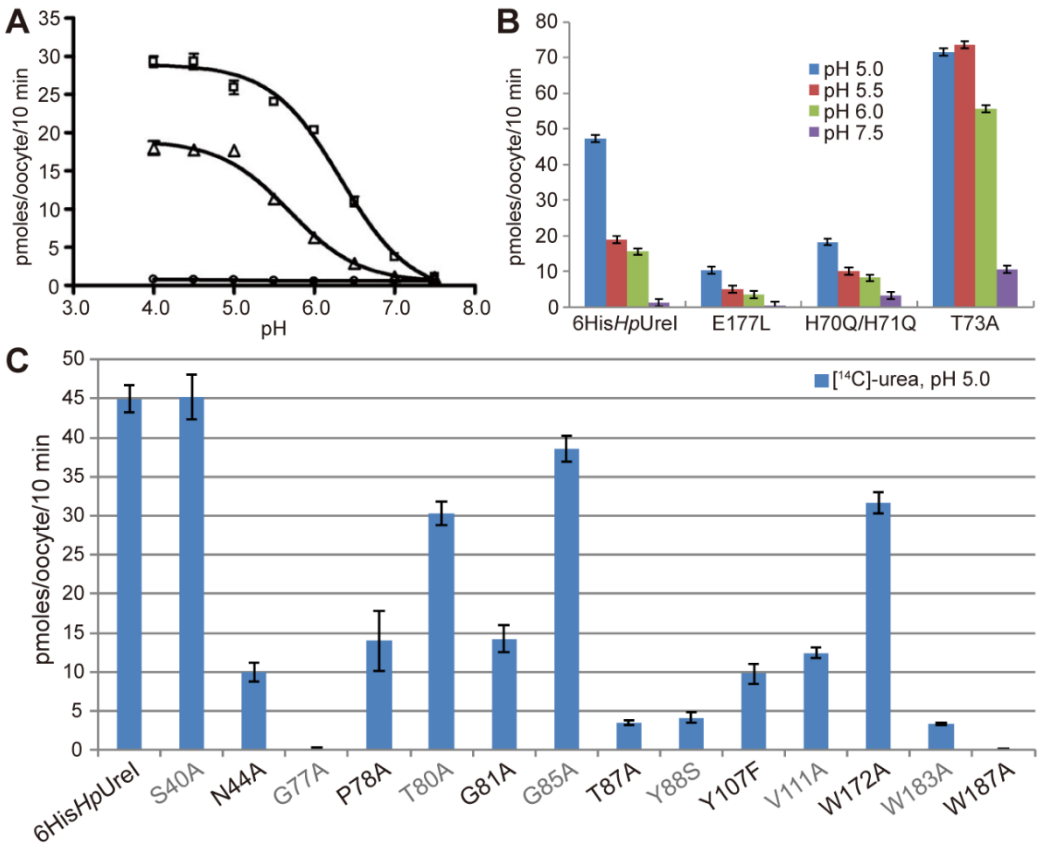

Fig. S8. Urea passage activity for wild-type *Hp*UreI and mutants of 6his*Hp*UreI. (**A**) Dependence of [^{14}C]-urea influx (pmol/oocyte/10 min) on pH for oocytes expressing wild type *Hp*UreI (□) or 6his*Hp*UreI (**Δ**) compared to non-injected control oocytes (○). (**B**) pH-dependence of [^{14}C]-urea influx (pmol/oocyte/10 min) for oocytes expressing 6his*Hp*UreI or mutants E177L, H70Q/H71Q, or T73A. (**C**) [^{14}C]-urea influx (pmol/oocyte/10 min) for oocytes expressing point mutants of 6his*Hp*UreI as compared to the control.

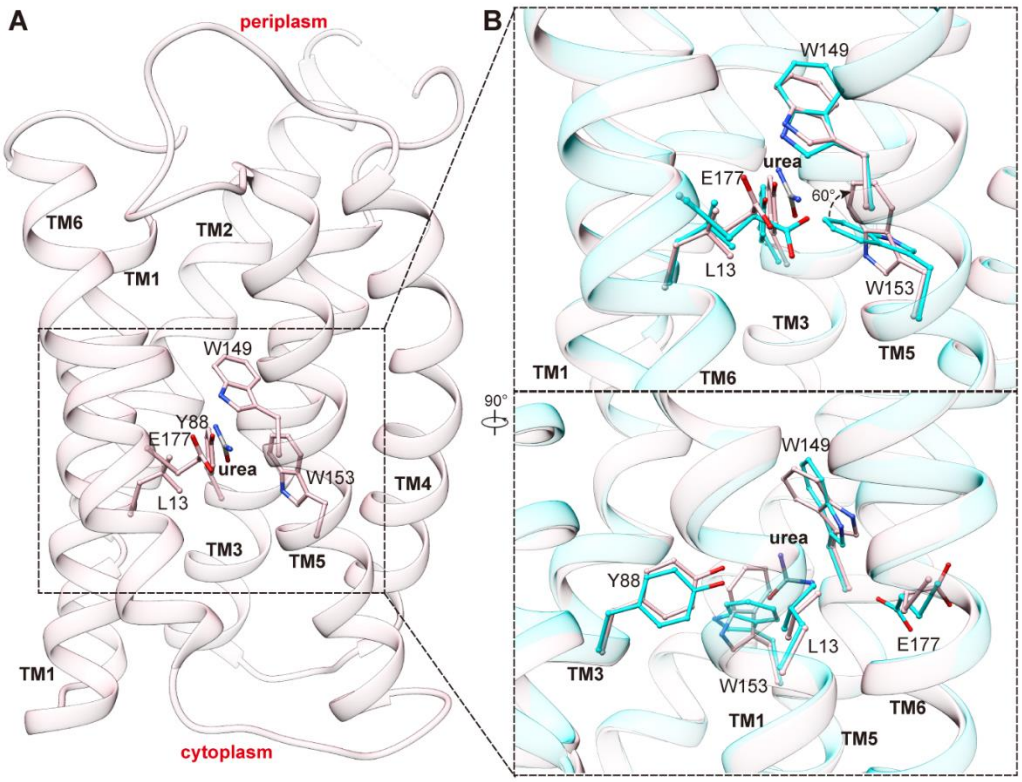

Fig. S9. Proposed filter model for urea fitted in the open conformation of 6his*Hp*UreI by using HADDOCK2.2. (**A**) Model for urea (grey) next to residues leu13, try88, trp149, trp153 and glu177 (sticks) in the proposed filter region of the 6his*Hp*UreI protomer (pink). **(B)** The same side chains from the original cryoEM model (cyan) compared to those of the model fitted with urea (pink).

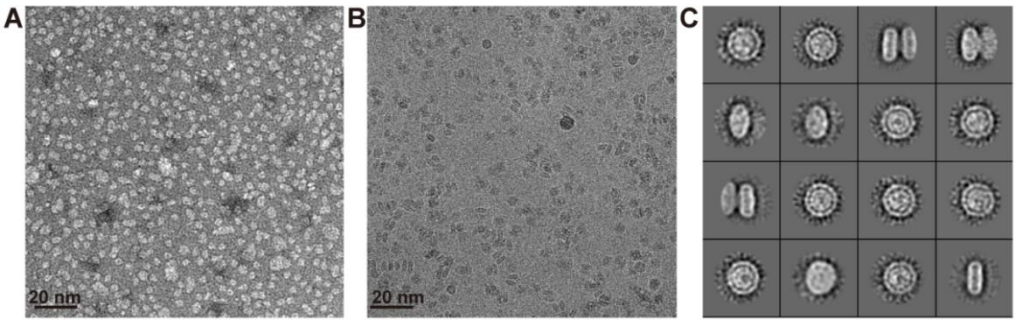

Fig. S10. Sample quality evaluation for 6his*Hp*UreI in DDM other than amphipol. (**A** and **B**) Representative negative stain (A) and cryoEM (B) micrographs of 6his*Hp*UreI in DDM. (**C**) Representative 2D class averages of particles from the cryoEM micrographs recorded from the sample in DDM showing poor structural features. Subsequent optimization of the sample in amphipol dramatically improved the visibility of the structural detail.

Table S1. Statistics of the cryo-EM structures.

	6his*Hp*UreI closed	6his*Hp*UreI open
CryoEM data collection and processing		
Microscope	**Krios**	**Krios**
Voltage (kV)	**300**	**300**
Nominal Magnification	**130,000**	**130,000**
Physical pixel size (Å)	**1.07**	**1.07**
Camera	**K2 summit**	**K2 summit**
Frame exposure time (s)	**0.15**	**0.15**
# movie frames	**100**	**60**
Total electron dose (e^-/Å^2)	**~72**	**~43**
Particle defocus range (μm)	**1.0-3**	**1.0-3**
# movies	**5,505**	**3,140**
# used movies	**4,026**	**2,901**
# extracted particles	**1,221,897**	**1,017,209**
# particles for 3D final maps	**393,930**	**279,840**
Symmetry for final maps	**C6**	**C6**
Resolution without mask (Å) / Map sharpening B-factor (Å^2)	**3.1 / -66.6**	**3.0 / -147.0**
Resolution with mask (Å) / Map sharpening B-	**2.7 / -71.9**	**2.7 / -89.5**

factor (Å^2)		
Atomic model refinement		
Number of protein residues	**1,092**	**1,092**
Number of atoms	**9,096**	**9,096**
RMSD bond lengths (Å)	**0.01**	**0.01**
RMSD bond angles (°)	**0.98**	**0.89**
MolProbity score	**1.99**	**1.31**
Clash score	**6.46**	**2.88**
Rotamer outliers (%)	**1.31**	**0**
Ramachandran statistics		
Most favored (%)	**94.01**	**97.10**
Additional allowed (%)	**5.99**	**2.90**
Outliers (%)	**0**	**0**

Movies Legends

Movie S1. Cryo-EM density views of 6his*Hp*UreI in closed conformation. 360° panorama of the density map, starting from periplasmic view. Protomers are colored separately and amphipol in grey.

Movie S2. Atomic model and density fit views of 6his*Hp*UreI in closed conformation. 360° panorama of the model, starting from periplasmic view. Protomers are colored separately.

Movie S3. Cryo-EM density views of 6his*Hp*UreI in open conformation. 360° panorama of the density map, starting from periplasmic view. Protomers are colored separately and amphipol in grey.

Movie S4. Atomic model and density fit views of 6his*Hp*UreI in open conformation. 360° panorama of the model, starting from periplasmic view. Protomers are colored separately.

Movie S5. 6his*Hp*UreI closed and open conformations morph. Morph movie, calculated using the "morph conformations" function in UCSF Chimera, of the closed and open states. This morph is not representative of the exact motion of the mechanism, but is intended to give a sense of scale for the dramatic conformational shift.